α SCALE SPACES FILTERS FOR PHASE BASED EDGE DETECTION IN ULTRASOUND IMAGES

Ahror Belaid ⋆ *Djamal Boukerroui* *

⋆Université Abderrahmane Mira de Béjaïa, Laboratoire d'Informatique Médicale (LIMED), 06000, Béjaïa, Algréie
*Université de Technologie de Compiègne - CNRS, Heudiasyc UMR 7253 BP 20529 - 60205 Compiègne Cedex, France

ABSTRACT

An inherent characteristic of coherent imaging, including ultrasound imaging, is the presence of speckle noise with strong inhomogeneities. It makes modelling difficult and therefore it complicates their processing. However, it has been previously shown that these images respond well to local phase-based methods. Furthermore, the recent re-emergence of the α scale spaces theory opens new possibilities of phase-based image processing. In this paper, we make use of this new unified representation to derive new families of bandpass quadrature filters. This construction leads to a generalised α kernel filters including the commonly known families derived from the Gaussian and the Poisson kernels. The properties of each family are first presented and then, experiments on realistic simulations of ultrasound images are shown to demonstrate how the suggested filters can be used for edge detection.

***Index Terms*—** α scale spaces, Quadrature filters, Edge detection, Local phase information, Ultrasound images.

1. INTRODUCTION

Ultrasound B-mode images are known to have low signal-to-noise ratio, low contrast, and high amounts of speckle, which is a correlated and multiplicative noise that inherently occurs in all types of coherent imaging systems. Moreover, ultrasound data often presents missing boundaries of the object of interest due to problems of specular reflection, shadows, signal dropout and attenuation. Consequently, ultrasound image segmentation is strongly influenced by the quality of data [1]. The literature on the subject is very abundant and interestingly edge based approches are well represented in this literature. Possibly because, as it has been pointed in [1], that echocardiography has been one of the driving application areas of medical ultrasound and the most popular approach to endocardial segmentation has been to treat it as a contour finding problem. Thus, in this study we focus on boundary detection on ultrasound images.

The extensive literature on the subject suggests that conventional intensity gradient-based methods have had limited success on typical clinical images [1], mainly because of low signal-to-noise ratio and also because of attenuation. Solutions using local phase information are successfully used in [2, 3, 4]. Indeed, phase based methods are theoretically intensity invariant and work better on ultrasound images.

The estimation of the local signal properties (local phase, amplitude and orientation) are based on the calculation of the analytical representation of the signal [5, 6]. However, a calculation of these local quantities cannot be done directly in a phase-based technique. In practice, it uses a pair of bandpass quadrature filters (an even filter and odd filter) [7]. What is quite certain is that the estimation is intrinsically noisy and depends critically on the choice of the quadrature filters pairs [8]. Furthermore, as these local properties are scale dependent, their use for feature detection requires also their scale invariance (at least in a certain range) in order to detect only salient features and not noise. Therefore, the only reasonable approach that has proven itself is to combine several scales. As mentioned earlier, this is in favour for the development of scale space representations and theories. It is in this double context of scale space and quadrature filters that Felsberg et al. [9, 10] have introduced the Monogenic Poisson scale space. This new theory opened new possibilities of phase-based image processing in scale space.

Recently, Duits et al. [11] worked on a generalised form of scale space filters, appeared initialy in [12], named the α scale spaces. It is a parameterised class ($\alpha \in]0; 1]$) of linear scale space representations which allows a continuous connection between the Poisson scale space (α = 1/2) and the well known Gaussian scale space (α = 1). In this paper, we make use of this new unified α scale space representation to derive new families of bandpass quadrature filters. These filters are built from derivatives and difference of the α scale space generating kernel. Thereby, they lead to the commonly known families of filters: Difference/Derivative of Poisson [10] and Gaussian filters. Following [8], the properties of each family are studied in terms of bandwidth, tuning frequency and unit normalisation constant. These definitions are presented in section 2. In section 3, we investigate the use of these filters for edge detection using the Monogenic Feature Asymmetry ($\mathrm{FA_M}$) measures [3]. A comparison with the Log-Gabor filter and preliminary results on simulated ultrasound images are also presented. Section 4 provides a discussion followed by some concluding remarks in section 5.

2. NEW BAND-PASS QUADRATURE FILTERS

Given a 1D real signal $f(x)$, its α scale spaces representation $v_s^{(\alpha)} : \mathbb{R} \times \mathbb{R}^+ \to \mathbb{R}$ is given by means of a convolution operation [11]:

$$v^{(\alpha)}(x,s) = \left(K_s^{(\alpha)} * f\right)(x) \ , \tag{1}$$

where s represents the scale parameter and $\alpha \in]0,1]$. The kernel $K^{(\alpha)}$ is defined in the Fourier domain by the following expression [11]:

$$\mathcal{K}^{(\alpha)}(\omega,s) = \exp\left(-s|\omega|^{2\alpha}\right) \ . \tag{2}$$

In the following section, we aim to derive two new quadrature families using the above generating kernel of the α scale space.

2.1. α scale spaces derivative filters

Following the same procedures as reported by Boukerroui et al. [8], we propose a new generalised formulation of a whole parameterised class of bandpass filters. This new family of filters is based on the derivatives of the generating kernel of the α scale space and leads to the Poisson derivatives (PoD) and the Gaussian Derivatives (GD) families. Thus, we define the following family of 1D α Scale Spaces Derivative (ASSD) quadrature filters in the frequency domain as follow:

$$\mathcal{F}_{ASSD}(\omega) = \begin{cases} n_c \omega^a \exp\left(-(s\omega)^{2\alpha}\right) & \text{if} \quad \omega \geq 0 \\ 0 & \text{otherwise} \end{cases} \tag{3}$$

where the derivative parameter $a \in \mathbb{R}^+$, meaning we are using fractional order derivatives. In order for the filters to satisfy the DC condition and to be also invariant to an additive ramp, we impose $a > 1$. n_c is a normalisation constant [8]. Important properties and tuning parameters of the ASSD filter, namely, the tuning frequency, filter's normalisations and the bandwidth, are given in the following propositions.

Proposition 2.1 *The peak tuning frequency of the scale space derivative filters is given by:*

$$\omega_0 = \frac{1}{s}\left(\frac{a}{2\alpha}\right)^{\frac{1}{2\alpha}} \ . \tag{4}$$

Proposition 2.2 *The unit normalisation constant n_c of the scale space derivative filters is given by:*

$$n_c = 2\frac{\sqrt{\pi\alpha}2^{\frac{2a+1}{4\alpha}} s^{a+\frac{1}{2}}}{\sqrt{\Gamma\left(\frac{2a+1}{2\alpha}\right)}} \ . \tag{5}$$

Proposition 2.3 *The octave bandwidth of the scale space derivative filters is given by:*

$$\beta = \frac{\ln\left(\frac{\mathcal{W}(-1,\mu)}{\mathcal{W}(0,\mu)}\right)}{2\alpha\ln(2)} \ , \mu = -\frac{1}{e2^{\frac{2\alpha}{a}}} \ . \tag{6}$$

where $\mathcal{W}(k,.)$ is the k^{th} branch of the Lambert function and $k = 0$ or -1.

2.2. Difference of α scale spaces filters

A second way to build a bandpass filter given a low pass filter, is to use the difference operator. Thus, we study a new generalised bandpass filter build from the Difference of two α Scale Spaces filters (DoSS). The impulse response of this new filter, in the frequency domain, is given by :

$$\begin{aligned}\mathcal{F}_{DoSS}(\omega) = n_c \exp\left(-\frac{1}{2}(s_1\omega)^{2\alpha}\right) \\ - n_c \exp\left(-\frac{1}{2}(s_2\omega)^{2\alpha}\right) \ ,\end{aligned} \tag{7}$$

where $\omega \geq 0$ and $s1 < s2$.

Proposition 2.4 *The peak tuning frequency of the difference of scale space filters is given by:*

$$\omega_0 = \frac{(4\alpha)^{\frac{1}{2\alpha}}}{s_2}\left(\frac{\log(\gamma)}{\gamma^{2\alpha}-1}\right)^{\frac{1}{2\alpha}} \quad \textit{with} \ \ \gamma = \frac{s_1}{s_2} \ . \tag{8}$$

Proposition 2.5 *The difference of scale space filters unit normalisation constant is given by:*

$$n_c = \frac{2\sqrt{\pi\alpha s_2}}{\sqrt{\Gamma(\frac{1}{2\alpha})}}\Big[1 + \frac{1}{\gamma} - 2\frac{2^{\frac{1}{2\alpha}}}{s_2^{2\alpha-1}(\gamma^{2\alpha}+1)}\Big]^{-\frac{1}{2}} \ . \tag{9}$$

Note that the bandwidth of the DoSS filter is evaluated numerically; see Fig. 1. Furthermore, observe that there is a common value, $\beta = 2.5$, that defines the ASSD filter's bandwidth almost for all values of α. This will be useful to set a common value for β during the experiments over all possible values of alpha.

3. APPLICATION TO EDGE DETECTION IN ULTRASOUND IMAGES

Our aim in this section is to investigate the behaviour of the proposed filters on contour detection. Specifically, we are

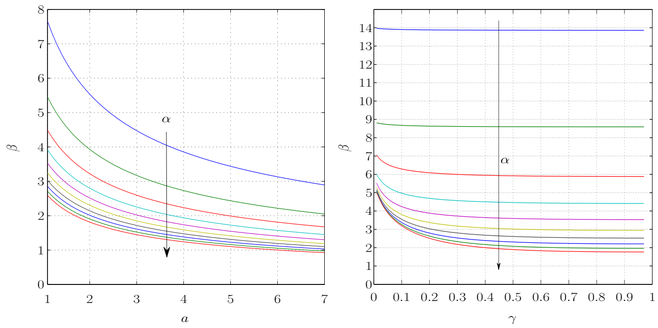

Fig. 1. Bandwidth of the ASSD filter as function of the derivative parameter a (left) and the DoSS filter as function of the scales ratio γ (right) for $\alpha \in \{0.1, 0.2, \cdots, 1\}$.

interested in the influence of the parameter α on the detection's performance. To this end, we use the *Monogenic Feature Asymmetry* ($\mathrm{FA_M}$) as a measure of contour detection. It is a phase based measure and uses multiple scales for the analysis of the given image.

3.1. The $\mathrm{FA_M}$ measures

The monogenic signal at a given scale s of a 2D signal $f(\mathbf{x})$ can be represented by a scalar valued even and a vector valued odd filtered responses, with the following simple tick:

$$\begin{aligned} even_s &= c * f \ , \\ \mathbf{odd}_s &= (c * h_1 * f, c * h_2 * f) \ , \end{aligned}$$

where c is the spatial domain representation of an isotropic bandpass filter tuned at scale s, and $\mathbf{h}(\mathbf{x}) = (h_1, h_2)(\mathbf{x}) = \frac{1}{2\pi}\frac{\mathbf{x}}{|\mathbf{x}|^3}$ is the generalised 2D Hilbert transform kernel [9, 10]. We define the multiple scales monogenic Feature Asymmetry by [3]:

$$FA_M = \frac{1}{N}\sum_s \frac{\lfloor |\mathbf{odd}_s| - |even_s| - t_s \rfloor}{\sqrt{even_s^2 + |\mathbf{odd}_s|^2 + \varepsilon}} \ , \qquad (10)$$

where N is the total number of scales, $\lfloor\cdot\rfloor$ denotes zeroing of negative values and t_s is a noise threshold estimated similarly as in [6].

3.2. Evaluation and results

The $\mathrm{FA_M}$ is evaluated on 120 realistic simulated ultrasound images with known ground truth. More details on these data can be found in [13], to which the reader is referred to. Some typical images are shown in Fig. 3. In our experimental study, the bandwidth β is set to $\{2.5, 3.6\}$ respectively for the ASSD and DoSS filters. 2.5 octaves is the only value possible for all $\alpha \in]0, 1]$, and 3.6 octaves is the lowest possible value for $\alpha \in]0.5, 1]$. We found by experiment that the wavelength of the finest scale $w = 12$ pixels was appropriate for most of our data. In order to detect fine as well as coarse structures, we consider three scales where the scaling factor between successive filters is set to 2.1.

The evaluation is carried out by comparing machine generated contours to ground-truth data using the *precision-recall* framework. In our context, the precision-recall curves are obtained by varying the detection threshold. There is an interesting point on this curve defined by the F measure, given as

$$F = 2\frac{Precision \cdot Recall}{Precision + Recall} \ .$$

Thus, the location of the maximum of the above measure along the curve defines the optimal threshold and provides a summary score. Herefore, following [14], we use the below quantities as evaluation scores: the best F cost on the dataset for a fixed scale (ODS)[1], the average F cost on the dataset for the best scale per image (OIS), and finally the average precision (AP) on the full recall range (equivalently, the area under the precision-recall curve).

Table 1. Results for $\mathrm{FA_M}$ contour detector using the ASSD, the DoSS and the Log-Gabor (LG) filters. Shown are the optimal value of α corresponding to the F-measure scores when choosing an Optimal Dataset Scale (ODS) or an Optimal Image Scale (OIS), as well as the Average Precision (AP). 120 simulated US images were used.

Filter	Parameter	ODS	OIS	AP
ASSD	$\alpha = 0.2$	0.69	0.71	0.54
DoSS	$\alpha = 0.9$	0.66	0.69	0.54
LG	$\beta = 3.6$	0.65	0.68	0.52

4. RESULTS AND DISCUSSION

Table 1 reports the main results of the contour detection experiments. More details, as well as the precision-recall curves of the results are shown in Fig. 2 (right). First, we notice that in general the results obtained by using the ASSD family outperforms significantly both the DoSS and the LG filters, and this for optimal values of α. Indeed, Fig. 2 shows that in a wide range, approximatively $\alpha \in]0, 0.85]$, the ASSD filters outperforms clearly the DoSS filters. While beyond $\alpha = 0.85$, the DoSS filters outperforms slightly the ASSD one. One reason for this may be the fact that the DoSS family have a larger bandwidth, since the lowest possible value in the range of $\alpha \in]0.5, 1]$ is 3.6 octaves. Therefore, it is more sensitive to noise and performs less on textured images. This observation is also supported by the few illustrative synthetic images shown in figures Fig. 3

Secondly, although the experimental study presented here is limited, it suggests that the ASSD filter with $\alpha = 0.2$ is more efficient (F=0.693) then the commonly used Gaussian

[1] Here we mean by scale, the detection threshold.

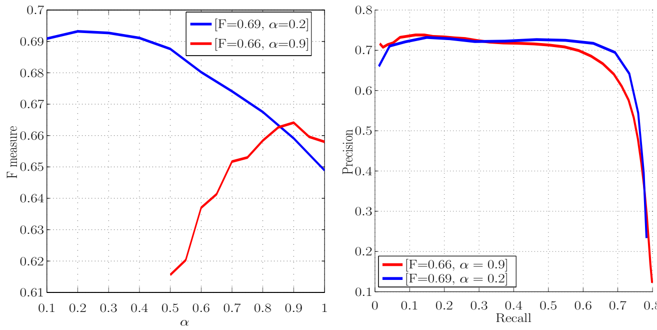

Fig. 2. F-measure as function of the shape parameter α (left) and Precision-Recall curves (right). The highest F-measure and the corresponding value of α are also reported for ASSD (blue line) and DoSS (red line) filters.

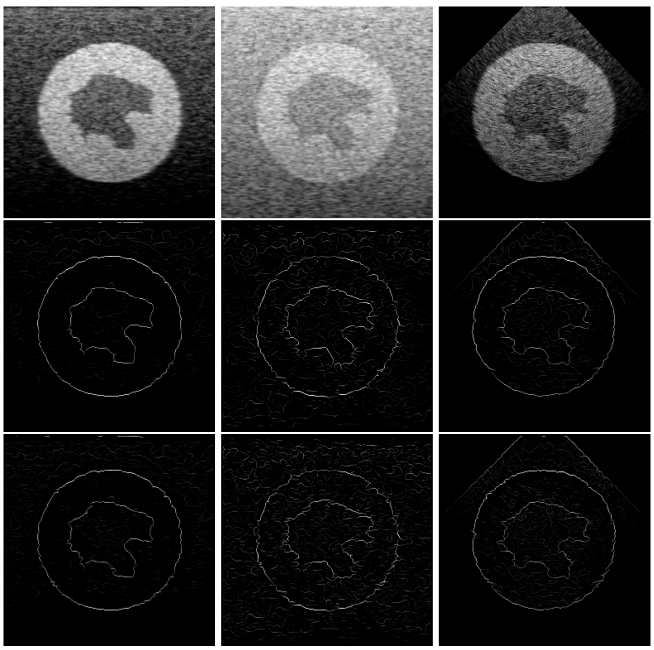

Fig. 3. Illustrative FA_M edge detection results using the ASSD and the DoSS filters on simulated US images with different: tissues characteristics, attenuation level and log compression parameters. From top to bottom: original images, edge detection using ASSD ($\alpha = 0.2$) and DoSS ($\alpha = 0.9$) filters respectively.

Derivative ($\alpha = 1$, F=0.648) and Poisson Derivative ($\alpha = 1/2$, F=0.687). Also, the DoSS filter with $\alpha = 0.9$ is more efficient (F=0.664) then Difference of Gaussian (F=0.658) and Difference of Poisson filters (F=0.615). Finally, the performances of the Log-Gabor filter seem to be close to the DoSS filter. This is confirmed by the close F measures in Table 1.

5. CONCLUSION

Two new parameterised classes ($\alpha \in]0; 1]$) of band-pass quadrature filters are presented. We then looked more closely at the influence of the shape parameter α in the context of phase based edge detection on ultrasound images. Based on a quantitative evaluation on 120 simulated images, the preliminary results show that the proposed ASSD and DoSS filters with specific values of α outperform the commonly used Log-Gabor and the special cases Derivative/Difference of Gaussian ($\alpha = 1$) and Poisson ($\alpha = 1/2$) filters.

6. REFERENCES

[1] J. A. Noble and D. Boukerroui, "Ultrasound image segmentation: A survey," *IEEE Trans. Med. Imag.*, vol. 25, no. 8, pp. 987–1010, 2006.

[2] M. Mulet-Parada and J. A. Noble, "2D+T acoustic boundary detection in echocardiography," *Med. Image Anal.*, vol. 4, no. 1, pp. 21–30, 2000.

[3] A. Belaid, D. Boukerroui, Y. Maingourd, and J-F. Lerallut, "Phase based level set segmentation of ultrasound images," *IEEE Trans. Info. Tech. Biomed.*, vol. 15, no. 1, pp. 138–147, 2011.

[4] A. Belaid, D. Boukerroui, Y. Maingourd, and J-F. Lerallut, "Implicit active contours for ultrasound images segmentation driven by phase information and local maximum likelihood," in *ISBI*, Chicago Illinois, USA, Apr. 2011, pp. 630–635.

[5] M. C. Morrone and R. A. Owens, "Feature detection from local energy," *Pattern Recognit. Lett.*, vol. 6, no. 5, pp. 303–313, 1987.

[6] P. Kovesi, "Image features from phase congruency," *Videre: J. Comput. Vis. Res.*, vol. 1, no. 3, pp. 1–26, 1999.

[7] H. Knutsson and M. Andersson, "Whats so good about quadrature filters," in *IEEE Int. Conf. Image Proc.*, 2003, pp. 61–64.

[8] D. Boukerroui, J. A. Noble, and M. Brady, "On the choice of band-pass quadrature filters," *J. Math. Imag. Vision*, vol. 21, no. 1, pp. 53–80, 2004.

[9] Michael Felsberg and Gerald Sommer, "Scale adaptive filtering derived from the laplace equation," in *Proc. of the 23rd DAGM-Symposium on Pattern Recognition*, London, UK, 2001, pp. 124–131, Springer-Verlag.

[10] M. Felsberg and G. Sommer, "The monogenic scale-space: A unifying approach to phase-based image processing in scale-space," *J. Math. Imag. Vision*, vol. 21, no. 1, pp. 5–26, 2004.

[11] Remco Duits, Michael Felsberg, Luc Florack, and Bram Platel, "α scale spaces on a bounded domain," in *Proc. Int. Conf. on Scale Space Methods in Computer Vision*, Berlin, Heidelberg, 2003, pp. 494–510, Springer-Verlag.

[12] E.J. Pauwels, L.J. Van Gool, P. Fiddelaers, and T. Moons, "An extended class of scale-invariant and recursive scale space filters," *IEEE Trans. Pattern Anal. Mach. Intell.*, vol. 17, no. 7, pp. 691–701, 1995.

[13] D. Boukerroui, "A local rayleigh model with spatial scale selection for ultrasound image segmentation," in *Proc. of British Machine Vision Conf.*, Surrey, UK, Sep 2012, pp. 84–84.

[14] P. Arbelaez, M. Maire, C. Fowlkes, and J. Malik, "Contour detection and hierarchical image segmentation," *IEEE Trans. Pattern Anal. Mach. Intell.*, vol. 33, no. 5, pp. 898–916, 2011.